The Influence of Non Uniform Heat Source and Thermal Radiation on the MHD Stagnation Point Flow of Maxwell Nanofluid Over a Linear Stretching Surface

Yasin Abdela[1], Bandari Shanker[2]
[1] Department of Mathematics, O.U, Hyderabad, 500-007, India.
[2] Professor of Mathematics, University College of Science, O.U, Hyderabad, 500-007, India.

Abstract: *In this article, the influence of non uniform heat source and thermal radiation on the MHD stagnation point flow of Maxwell nanofluid over a linear stretching surface is reported. An appurtenant similarity transformation has been applied to transform the governing equations in partial differential equations form into the non linear ordinary differential equation form. The transformed equations are solved using the fourth order Runge-Kutta method. The flow behaviors, heat and mass transfer features have been discussed besides the results are supported graphically and in tabular form. The effect of pertinent and sundry parameters on velocity, temperature and concentration profiles are shown through graphs and the values of the skin coefficient, local Nusselt number and local Sherwood numbers are tabulated.*

Key words: *Linear stretching surface, MHD, Stagnation point flow, Maxwell Nanofluid and Non uniform heat source/sink.*

Nomenclature:

a	Velocity of the stretching surface
b	Free Stream velocity
T	Temperature of the fluid in the boundary layer
C	Concentration of the fluid in the boundary layer
T_w	Stretching surface temperature
C_w	Stretching surface concentration
T_∞	Ambient fluid temperature
C_∞	Ambient fluid concentration
u	Velocity component along the x- axis
v	Velocity component along the y- axis
u_w	Velocity component along the x- axis at the wall
v_w	Velocity component along the y- axis at the wall
υ	Kinematic viscosity
τ	The effective heat capacity of the Nanoparticle to the heat capacity of the fluid
$(\rho c)_p$	Effective heat capacity of Nanoparticle material
$(\rho c)_f$	Effective heat capacity of the Fluid
α	Thermal diffusivity
σ^*	Stefan-Boltzmann constant
D_B	Brownian diffusion coefficient
D_T	Thermophoresis diffusion coefficient
k_1	Thermal conductivity
k	Maxwell parameter
k^*	Mean absorption coefficient
M	Magnetic field parameter
Pr	Prandtl number

Nb	Brownian motion parameter
Nt	Thermophoresis parameter
A^*	The space dependent heat source/sink Parameter
B^*	The Temperature dependent heat source/sink Parameter
R	Radiation parameter
Le	Lewis number
λ	Velocity ratio parameter
Cf_x	Local skin friction
Nu_x	Local Nusselt number
Sh_x	Local Sherwood number

1. Introduction:

Nanofluids are two phase mixtures involving base fluid and small particles with size less than 100 nm suspended within them. In most cases the base fluids used are water, oil, glycol, polymeric solutions etc and the materials used for nanoparticles are like alumina, silica, diamond graphite, Alo3, Cuo, Ag, and Cu. Efficiently engineered nanofluid provides high specific surface area that allows to have more heat transfer surface between particles and fluids, more stable dispersions of the nanoparticles, minimized particles clogging, adjustable properties such as thermal conductivity by varying particle concentration, the collision and interaction among particles, the surface of the flow passage and base fluids are intensified. Viscoelastic fluids are time dependent non-Newtonian fluids which behave both viscous and elastic. Maxwell fluid is one of the viscoelastic fluids.

In fluid dynamics a stagnation point is a point in a flow field where the local velocity of the fluid is zero.
Stagnation point exists at the surface of object in the flow field, where the fluid brought to rest by the object. The Bernoulli equation shows that the static pressure is highest when the velocity is zero hence the static pressure attains its maximum value at the stagnation point.Stagnation point flow represents a fluid flow in the immediate neighborhood of solid surface at which fluid approaching the surface divides into different streams. Although the fluid is stagnant everywhere on the solid surface due to no-slip boundary condition.
The stagnation point flow of nanoviscoelastic fluids over a linear stretching surface is the most applicable study in technology and manufacturing industries. Some of the applications are polymer foams used in seat cushion creep, Guitar strings are viscoelastic, and viscoelastic dampers are used in tall buildings to absorb vibration energy due to earth quakes. It is used in pneumatic drills and makes to line the gloves worn by people. Viscoelastic materials are excellent impact observers such as a peak impact force can be reduced by a factor of two if impact buffer is made of viscoelastic rather than elastic. Elastomers are highly viscoelastic and make good impact observers. Moreover viscoelastic materials are used in automobile bumpers, on computer derives to protect mechanical shakes, in helmets (foam padding inside) wrestling mats shoe soles etc. It is because of this extensive application of the stated flow that many investigators have been dealing with the stagnation point flow of nanoviscoelastic fluids over a linear stretching surface.

Ahmed [1] has shown the effect of slip velocity on the heat transfer and the flow pattern on Maxwell fluid of the unsteady flow over a stretching sheet in the presence of the variable heat flux and fluid properties of the Maxwell fluids. Awan et al. [2] have determined the analytical solution for the velocity and adequate shear stress corresponding to the longitudinal flow of a fraction of Maxwell fluid between two infinite coaxial circular cylinders. Dumirtru and Azhar [3] have concluded that the fluid flow properties of coutte flow of Maxwell fluid by comparing the velocity field corresponding to both flows with slip and no slip boundary conditions for Maxwell and Newtonian fluids. They have determined the relative velocity of the bottom plate translates with the constant velocity, the velocity corresponding to the four types of the flows were written as the sums between the stationary solution and the transient solution. Emilia and Ivan [4] have considered the Stokes first problem for a class of viscoelastic fluids with the generalized fractional Maxwell constitutive model. They have explicitly derived on integral representation of the solution and some characteristics like non negativity and monotonicity asymptotic behavior analyticity, finite/infinite propagation speed and absence of wave front have discussed. Ramesh et al. [5] have studied the stagnation point flow of Maxwell fluid towards a permeable stretching in the presence of nanoparticles. They have concluded that the velocity boundary layer is formed for λ >1 (the velocity ratio is greater than one) and the inverse one is formed when λ <1 and the relaxation time k and $f''(0)$ have the same direction but k and $-\phi'(0)$ go on opposite direction where as k and $-\theta'(0)$ have the same direction for $\lambda<1$ but opposite for $\lambda>1$. Ramesh and Gireesha [6] have investigated the effect of heat source/sink on the steady boundary layer flow of Maxwell fluid over a stretching sheet with convicted boundary conditions in the presence of nanoparticles and have found that Nusselt number is smaller and Sherwood number is higher for Maxwell fluids compared with Newtonian fluids. Josephe [7] has verified the conjectures of stagnation point flow of an upper convicted Maxwell fluid derived by the other investigators and has proved the solution has monotonically increasing first derivative. Rosenberg and Keunings [8] have examined further results on the flow of Maxwell fluid through an abrupt contraction and suggested that the limit point is an intrinsic property of the Maxwell fluid and for numerical solutions obtained at values of weissenberg number close to the limit point show spurious wiggles near the corner. Vander et al. [9] have solved the upper convicted Maxwell model of an elastic liquid using finite element and have shown that the algorithm produces oscillations in the stress in the presence of geometrical discontinuities for increased Deborah number. Abro and Shaikh [10] have analyzed the velocity field properties and the adequate shear stress of the Maxwell fluid moving with no slip effects over an infinite plate and have indicated that when the relaxation time approaches to zero, then the models will be reduced to Newtonian fluid. Boubaker [11] has extended the classical Maxwell model for viscoelastic fluids in terms of characteristic relations time strain dependence and it is very useful in describing the response of geological and many other polymeric solutions. Key-chyang Lee and Bruce [12] have reported that for the poiseuille flow problem Eigen modes that are anti-symmetric in position. They have considered augmenting the literature results for the symmetric Eigen modes and have concluded that the symmetric and anti-symmetric modes are more dangerous when the wave number and weissenberg number are large and no unstable Eigen values are found. Sekhar et al [13] have studied the flow and heat transfer characteristics of Sakiadis and Blasius flow of MHD Maxwell fluid with the effect of exponentially varying heat source/sink. They have reported that heat transfer is very high in Blasius flow as compared to the Skiadis flow and heat generation parameter depreciates both the momentum and thermal boundaries layer thickness. Vajravelu et al [14] have investigated the MHD flow and mass transfer of an upper convicted Maxwell fluid with homogeneous-heterogeneous reactions and found that the velocity distribution decreases with the increase of both the magnetic parameter and the Maxwell parameter. Liku and Ahmed [15] have examined the peristaltic of fractional generalized Maxwell viscoelastic fluid through a porous medium. They have revealed that the bolus formed were trapped by wave and the size of trapping bolus reduces when the magnitudes of the permeability parameter and slip parameter increases. Macha et al. [16] have presented the effect of thermal radiation on the unsteady MHD boundary layer flow of non-Newtonian Maxwell nanofluid over a stretching surface and have studied the effect of each governing parameter involved in the problem. Meraj and Junaid [17] have investigated the flow of Maxwell nanofluid over a moving plate in a calm fluid and found the variation in velocity distribution with the increase in local Deborah number is non monotonic and reduced Nusselt number and Deborah number have linear and direct relation. Mustafa et al.[18] have explored the influence of non uniform transverse magnetic field on the flow of Maxwell fluid due to constantly moving flat radiative surface with convective conditions and they have found that variation in velocity with an increase in local Deborah number is non monotonic where as temperature is decreasing function of local Deborah number. Qasim and Noreen [19] have studied the effect of non uniform applied magnetic field on the Falkner-Skan flow of Maxwell fluid and found that increasing the Deborah number decreases the boundary layer thickness of the velocity and the temperature profile increases with the increase of the Hartman number as well as they have studied the effect the other parameters on the properties of the flow and heat transfer. Nazaila [20] has dealt with the influence of thermal radiation on stagnation point flow past a stretching/shrinking sheet in a Maxwell fluid with slip conditions and examined the features of the flow and heat transfer characteristics for the different parameters involved in the problem. Halim [21] has investigated the steady stagnation point flow of an incompressible Maxwell fluid towards a linearly stretching sheet with active and passive control of the nanoparticles and has found that temperature distribution in passive control model are consistently lower than in active control model. Noor et al. [22] have explored the effect of heat absorption and thermal radiation in non Newtonian fluid on a vertical stretching sheet with suspended particles and found that the heat flux of the flow is uplifted as value of either heat absorption or thermal radiation is multiplied. Noor [23] has presented the study of MHD flow of Maxwell fluid past a vertical stretching sheet with thermophoresis and chemical reaction and revealed that as the value of thermophoresis, chemical reaction parameters and Schmidt number escalated the thickness of the mass boundary layer declines. Sandeep and Sulochana [24] have dealt with the effect of non uniform heat source/sink thermal radiation suction on the momentum and transfer behaviors' of Jeffrey, Maxwell and oldroyd-B nanofluid over stretching surface. They have shown that the rise in the value of magnetic parameter reduces the friction factor and increase on non uniform heat source/sink and the thermal radiation increases the temperature profiles of the flow. Syed and Veera [25] have reported the flow of incompressible viscous Maxwell fluid between two parallel plates induced by constant pressure gradient and found that the magnitude of velocity enhances with increase in both the Reynolds number and the Maxwell fluid parameter and reduces with the increase of pressure. Siddique [26] has studied the longitudinal flow of the generalized Maxwell fluid in an infinite circular cylinder due to the longitudinal variable time dependent shear stress that is prescribed on the boundary of the cylinder. SinWeingWong et al. [27] have analyzed the study of two dimensional stagnation point flow of an incompressible fluid towards a stretching vertical sheet and found that dual solution in the opposing buoyant flows but the solution is unique for the assisting buoyant flows. Sreekala et al.[28] have investigated the unsteady MHD flow of electrically conducting Maxwell fluid in a parallel plate channel bounded by porous medium under the influence of uniform magnetic field inclined at an angle of inclination with the normal to the boundaries. Swati [29] has studied unsteady two dimensional flow of a Maxwell fluid over a stretching surface in a porous medium subjected to suction/blowing and has found that the fluid velocity initially decrease with the increase of unsteadiness parameter and the velocity decreases with the increase of permeability parameter. Swati [30] has reported on the unsteady two dimensional flow of MHD non Newtonian Maxwell fluid over a stretching surface with a prescribed surface temperature in the presence of heat source/sink and revealed temperature decreases significantly due to unsteadiness. Hayat et al. [31] have explored the steady two dimensional MHD flow of an upper convicted Maxwell fluid near a stagnation point over a stretching surface and concluded that the velocity decrease with increase of the Deborah number and Hartman number while the skin friction coefficient increase with the increase of both. Hayat et al. [32] have dealt with the three dimensional flow of Maxwell fluid over a stretching surface with convective boundary condition and have shown that the Deborah and Biot parameters are opposite on Nusselt number where as the Prandtl and Biot numbers have qualitative similar impact on the Nusselt number. Vijendra and Shweta [33] have examined the MHD flow and heat transfer for Maxwell fluid over an exponentially stretching sheet through a porous medium in the presence of non uniform heat source/sink with thermal conductivity. Abbas et al. [34] have investigated the steady convection boundary layer flow of an incompressible Maxwell fluid near the two dimensional stagnation point flow over a vertical stretching surface. They have proved the results using comparisons of the results obtained by the two different methods.

From the literatures given above, one can easily understand that a number of investigations have been conducted on the stagnation point flow of Maxwell fluids over a linear stretching surface. According to the knowledge of the author's the influence of non uniform heat source/sink and thermal radiation on the MHD stagnation point flow of Maxwell nanofluid over a linear stretching surface not yet investigated. Therefore in the present paper, we have dealt with the influence of non uniform heat source/sink and thermal radiation on the MHD stagnation point flow of Maxwell nanofluid over a linear stretching surface. The governing equations are transformed into Non-linear ordinary differential equations using suitable similarity transformation and the results are solved numerically using the fourth order Range-Kutta method. We investigated the effect of the relevant parameters using several set of values of the parameters and the results are analyzed for the flow, heat and mass transfer characteristics.

2. Mathematical formulation:

The steady incompressible, two dimensional stagnation point flow of Maxwell nanofluid over a linear stretching surface that coincides with the plane y=0 is considered and the flow is carried out at $y \geq 0$, where y is the coordinate measured normal to the stretching surface. Two equal and opposite forces are applied along the x-axis so that the surface is stretched keeping the origin fixed. A constant magnetic field of strength B_0 acts in the direction of the y-axis. The induced magnetic field is negligible, which is a valid assumption on laboratory scale under the assumption of small Reynolds number. It is also assumed the external electric field is zero. Consider the velocity of the stretching surface to be $u_w(x) = bx$ and the velocity of the free stream flow to be $u(x) = cx$, where b and c are positive constants and x is the coordinate measured along the stretching surface. Assume that T_w, C_w are the temperature and concentration at the stretching surface respectively while T_∞, C_∞ be the ambient temperature and ambient concentration respectively.

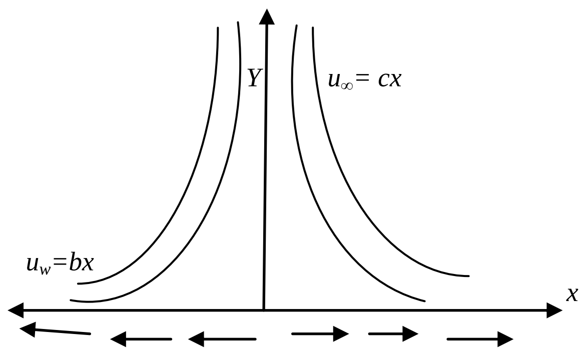

Figure 1 physical sketch of the problem

Taking the above assumptions into consideration and using the Maxwell model as it is described in [31], the governing equations for the boundary layer motion, energy and concentration in the presence of non uniform heat source/sink, thermal radiation and viscous dissipation are stated below.

$$\frac{\partial u}{\partial x}+\frac{\partial v}{\partial y}=0 \qquad (1)$$

$$u\frac{\partial u}{\partial x}+v\frac{\partial u}{\partial y}+\lambda_1\left(u^2\frac{\partial^2 u}{\partial x^2}+v^2\frac{\partial^2 u}{\partial y^2}+2uv\frac{\partial^2 u}{\partial x\partial y}\right)=\upsilon\frac{\partial^2 u}{\partial y^2}+U\frac{\partial U}{\partial x}-\frac{\sigma B_0^2 u}{\rho} \qquad (2)$$

$$u\frac{\partial T}{\partial x}+v\frac{\partial T}{\partial y}=\alpha\frac{\partial^2 T}{\partial y^2}+\tau\left[D_B\frac{\partial C}{\partial y}\frac{\partial T}{\partial y}+\frac{D_T}{T_\infty}\left(\frac{\partial T}{\partial y}\right)^2\right]+\frac{q'''}{\rho c_p}-\frac{1}{\rho c_p}\frac{\partial q_r}{\partial y} \qquad (3)$$

$$u\frac{\partial C}{\partial x}+v\frac{\partial C}{\partial y}=D_B\frac{\partial^2 C}{\partial y^2}+\frac{D_T}{T_\infty}\frac{\partial^2 T}{\partial y^2} \qquad (4)$$

Under the Rosseland approximation the radiative heat flux as given [17] has the form

$$q_r=\frac{4\sigma^*}{3k^*}\frac{\partial T^4}{\partial y} \qquad (5)$$

Where σ^* is the Stefan-Boltzmann constant and k^* is the mean absorption coefficient. Assume that the temperature difference in the flow be adequately small so that T^4 may be expressed as a linear function of temperature. Using the Taylor series expanding T^4 excluding the higher order terms result in

$$q'''=\frac{k_1 u_w}{x\upsilon}[A^*(T_w-T_\infty)f'+B^*(T-T_\infty)] \qquad (6)$$

Using (6) in (5) $T^4\cong 4T_\infty^3 T-3T_\infty^4=T_\infty^3(T-T_\infty)$ we get

$$\frac{\partial q_r}{\partial y}=-16\sigma^* T_\infty^3\frac{\partial^2 T}{\partial y^2}$$

q''' is the space and temperature dependent heat source/sink that is defined as [25]

Where u and v are the velocity components along x and y directions respectively, υ is the kinematic viscosity, α is the thermal diffusivity, τ is the effective heat capacity of nanoparticle to the heat capacity of the fluid, D_B is the Brownian motion coefficient, D_T is the thermophoresis diffusion coefficient, A* and B* are the parameters of the space and temperature dependent internal heat source/sink. If A*>0, B*>0, it represents heat is generated and A*<0,B*<0 it represents heat is absorbed The corresponding boundary conditions are

$$\left.\begin{array}{lllll} u = bx & v = 0 & T = T_w & C = C_w & at \quad y = 0 \\ u = cx = U & & T \to T_\infty & C \to C_\infty & as \quad y \to \infty \end{array}\right\} \tag{7}$$

The similarity transformation employed is the one that is stated in [22].

$$\left.\begin{array}{lll} \eta = \sqrt{\dfrac{b}{\upsilon}}y, & u = bxf'(\eta), & v = -\sqrt{\upsilon b}\, f(\eta) \\ \theta = \dfrac{T - T_\infty}{T_w - T_\infty} & \phi = \dfrac{C - C_\infty}{C_w - C_\infty} & \end{array}\right\} \tag{8}$$

Applying (8) on (2), (3), (4) yield

$$(1 - kf^2) f''' + 2kf\, f' f'' + f\, f'' - f'^2 - Mf' + \lambda^2 = 0 \, , \tag{9}$$

$$(3R + 4)\theta'' + 3\,\mathrm{R}\,\mathrm{Pr}\left(f\theta' + Nb\phi'\theta' + Nt\theta'^2 \right) + 3R\left(A^* f' + B^*\theta \right) = 0 \tag{10}$$

$$\phi'' + Lef\phi' + \frac{Nt}{Nb}\theta'' = 0 \tag{11}$$

The boundary conditions are given below.

$$\left.\begin{array}{llll} f'(0) = 1 & \theta(0) = 1 & \phi(0) = 1 & at \ \eta = 0 \\ f' \to \lambda & \theta \to 0 & \phi \to 0 & \text{as} \ \eta \to \infty \end{array}\right\} \tag{12}$$

Where the primes are derivatives with respect to η , the velocity ratio parameter is $\lambda = \frac{c}{b}$, the magnetic field parameter is $M = \frac{\sigma\beta_0^2}{b}$, the Maxwell parameter (the relaxation time parameter) is $k = b\lambda_1$, The prandtl number is $\Pr = \frac{\upsilon}{\alpha}$, the Lewis number is $Le = \frac{\upsilon}{D_B}$, the radiation parameter is $R = \frac{kk^*}{4\sigma^* T_\infty^3}$,the Brownian motion parameter is $Nb = \frac{D_B (C_w - C_\infty)}{(\rho_c)_f \upsilon}$, the thermophoresis parameter is $Nt = \frac{(\rho_c)_p D_T (T_w - T_\infty)}{(\rho_c)_f \upsilon T_\infty}$ and $\tau = \frac{(\rho_c)_p}{(\rho_c)_f}$

It is known that Nb and Nt contains the x-coordinate and therefore it is must to look for the variability of the local similarity solution that gives chances to investigate the behavior of these parameters at affixed location above the sheet. The skin friction coefficient Cf_x , the local Nusselt number Nu_x and the local Sherwood number Sh_x as they are described in [17] are stated below.

$$Cf_x = \frac{\mu\left(\frac{\partial u}{\partial y}\right)_{y=0}}{\rho u_w^2}, \quad Nu_x = \frac{-x\left(\frac{\partial T}{\partial y}\right)_{y=0}}{T_w - T_\infty}, \quad Sh_x = \frac{-x\left(\frac{\partial C}{\partial y}\right)_{y=0}}{C_w - C_\infty} \tag{13}$$

Employing the similarity transformation (8) on (13) we get

$$\mathrm{Re}_x^{\frac{1}{2}} Cf_x = f''(0), \quad \frac{Nu_x}{\mathrm{Re}_x^{\frac{1}{2}}} = -\theta'(0), \quad \frac{Sh_x}{\mathrm{Re}_x^{\frac{1}{2}}} = -\phi'(0) \tag{14}$$

2. Method of Solution:

The numerical fourth order Runge-Kutta method along with shooting technique is employed to solve the coupled ordinary differential equations (9) (10) and (11), with their allied boundary conditions (12) as it is employed in [6]. The system of non linear higher order differential equations (9),(10) and(11) should be changed into a system of first order differential equations in order to employ the method described. To transform the system of non linear higher order differential equations into a system of first order differential equations we apply the notations below.

Let

$$\left.\begin{aligned} &f = f(1), \quad f' = f(2), \quad f'' = f(3) \\ &\theta = f(4), \quad \theta' = f(5) \\ &\phi = f(6), \quad \phi' = f(7) \end{aligned}\right\} \tag{15}$$

Applying equations (15) in equations (9),(10) and(11) we have

$$\left.\begin{aligned}
f''' &= -\frac{2k}{1-kf^2} ff'f'' - \frac{1}{1-kf^2} ff'' + \frac{1}{1-kf^2} f'^2 + \frac{Mf'}{1-kf^2} - \frac{\lambda^2}{1-kf^2} \\
&= -\frac{2*k}{1-k*f(1)*f(1)} f(1)*f(2)*f(3) - \frac{1}{1-k*f(1)*f(1)} f(1)*f(3) \\
&\quad + \frac{1}{1-k*f(1)*f(1)} f(2)*f(2) + \frac{M*f(2)}{1-k*f(1)*f(1)} - \frac{\lambda^2}{1-k*f(1)*f(1)} \\
\theta'' &= -\frac{3R\,\mathrm{Pr}}{3R+4}[Nb\phi'\theta' + f\theta' + Nt\theta'^2] - \frac{3R}{3R+4}[A^* f' + B^*\theta] \\
&= -\frac{3*R*\mathrm{Pr}}{3*R+4}[Nb*f(7)*f(5) + f(1)*f(5) + Nt*f(5)*f(5)] \\
&\quad - \frac{3*R}{3*R+4}[A^* * f(2) + B^* * f(4)] \\
\phi'' &= -Le\phi' f - \frac{Nt}{Nb}\theta'' \\
&= -Le*f(7)*f(1) + \frac{3*Nt*R*\mathrm{Pr}}{Nb*(3*R+4)}*[Nb*f(7)*f(5) + f(1)*f(5) + Nt*f(5)*f(5)] \\
&\quad - \frac{3*Nt*R}{Nb*(3*R+4)}*[A^* * f(2) + B^* * f(4)]
\end{aligned}\right\} \tag{16}$$

The corresponding boundary conditions are

$$\left.\begin{array}{llll} f_a(1)=0, & f_a(2)=1, & f_a(4)=1, & f_a(6)=1 \\ f_{b'}(2)\to\lambda, & f_{b'}(4)\to 0 & & f_{b'}(6)\to 0 \\ \text{where } a=0 & & & \text{and } b'=\infty \end{array}\right\} \quad (17)$$

$f''(0), \theta'(0)$ *and* $\phi'(0)$ are not given in the boundary conditions of the system of the ordinary differential equations. Therefore, we calculate the approximate values $f''(0), \theta'(0)$ *and* $\phi'(0)$ using the shooting technique first and then we apply the fourth order Runge-Kutta method to get f, θ *and* ϕ. We choose the step size to be $\Delta h = 0.01$ with accuracy of 10^{-5}.

3. Results and discussions:

The impact of the sundry parameters intricate in the coupled ordinary differential equations such as the velocity ratio λ ,the Maxwell parameter k, the magnetic field parameter M, the prandtl number Pr, the thermal radiation parameter R, the Brownian motion parameter Nb, the thermophoresis parameter Nt, the space dependent and temperature dependent heat source/sink parameters respectively A^* and B^* and the Lewis number Le on the stagnation point flow of Maxwell nanofluid over a linear stretching surface have been discussed with the help of their graphs and tabulated values.

Table1. Table of comparison for skin friction coefficient $f''(0)$ for different values of λ

λ	Hayat $f''(0)$	Ramesh et al.[6] $f''(0)$	Present result of $f''(0)$
0.01	-0.9982	-0.9991	-0.998028
0.1	-0.9695	-0.9696	-0.969386
0.2	-0.9181	-0.9181	-0.918107
0.5	-0.6673	-0.6672	-0.667264
2.0	2.0176	2.0175	2.017487
3.0	4.7296	4.7292	4.729182

Table2. For the different values of λ comparison of the local Nusselt number $-\theta'(0)$.

Pr	λ	Hayat $-\theta'(0)$	Ramesh et al.[6] $-\theta'(0)$	Present result of $-\theta'(0)$
1	0.1	0.6021	0.6048	0.601814
	0.2	0.6244	0.6256	0.624131
	0.5	0.6924	0.6925	0.692111
2	0.1	0.7768	0.7769	0.776373
	0.2	0.7971	0.7971	0.796700
	0.5	0.8647	0.8647	0.864374

Table3. Comparison table of the local Nusselt number $-\theta'(0)$ in the absence of Maxwell

Parameter and the velocity ratio.

Nt	Nb=0.1		
	Khan and Pop $-\theta'(0)$	Ramesh et al.[6] $-\theta'(0)$	Present result of $-\theta'(0)$
0.1	0.9524	0.9523	0.953984
0.3	0.5201	0.5200	0.523873
0.5	0.3211	0.3210	0.324461

The present results for the considered velocity ratio parameter λ in table1 above agree to three decimal places with the results of Ramesh et al. [6]. Therefore the results have excellent agreement. In table 2 above, for the given values of the velocity ratio parameter λ and the Prandtl number Pr the present result agree to two decimal places with the results communicated by Ramesh et al. [6] and hence the results have very good agreement. In table 3 above, for the given values of the Brownian motion parameter Nb and the thermophoresis parameter Nt the present result agree to two decimal places with the results reported by Ramesh et al. [6] and hence the results have very good agreement.

In table 4 below as the values of the Maxwell parameter k enlarged from 0.01 to 0.03, the velocity of the fluid and the boundary layer thickness decreased. In the second part of table 4 the velocity and the boundary thickness diminished with the increment of the magnetic field parameter. The velocity of the fluid and the boundary layer thickness escalated with the enlargement of the velocity ratio $\lambda = \frac{b}{c}$ <1 (i.e. the velocity of the stretching surface is greater than the free stream velocity) as it is indicated in the third part of table 4. The Nusselt number increases as the prandtl number increases so that the thermal boundary layer thickness declines as it is shown in the fourth part of table 4. In the fifth, sixth and seventh parts of table 4 enhancing Nb, Nt and R decreases the Nusselt number and thicken the boundary layer. In the 8th and 9th parts of table 4 increasing A* and B* result in the increase of the generation of thermal energy. So that the nanofluid temperature enlarged and this causes the reduced Nusselt number to descend and the Sherwood number to ascend. In the last part of table 4 the Nusselt number decreases and the Sherwood number increases with the increase of Lewis number. Because the larger the Lewis number the weaker molecular diffusivity and the thinner concentration boundary layer.

Table 4

Numerical results of $f''(0), -\theta'(0), and\ -\phi'(0)$ for different values the parameters involved.

k	M	λ	Pr	Nb	Nt	R	A^*	B^*	Le	$-f''(0)$	$-\theta'(0)$	$-\phi'(0)$
0.01	0.05	0.05	1	0.01	0.01	1	0.01	0.01	1	0.847340	0.413077	0.50924
0.02										0.855725	0.410989	0.506257
0.03										0.861912	0.409567	0.504184
0.05	0.01	0.05	1	0.01	0.01	1	0.01	0.01	1	0.823396	0.418661	0.513271
	0.02									0.829885	0.417929	0.512489
	0.03									0.844651	0.414260	0.508500
0.05	0.05	0.1	1	0.01	0.1	1	0.01	0.01	1	0.857638	0.411059	0.505059
		0.5								0.635698	0.439891	0.536499
		0.7								0.433127	0.462272	0.560586
0.2	0.2	0.2	2	0.01	0.1	0.3	0.1	0.1	5	0.887310	0.42128	0.655761
			3.5							0.887221	0.462133	0.465955
			4							0.835739	0.514844	0.307383
0.2	0.2	0.2	1	0.1	0.01	0.5	0.01	0.01	3	1.133793	0.143357	0.884691
				0.3						1.133793	0.138305	0.814294
				0.5						1.133793	0.133420	0.800205
0.2	0.2	0.2	1	0.01	0.1	0.5	0.1	0.1	3	0.887187	0.219192	1.037212
					0.3					0.887214	0.213535	0.748720
					0.5					0.887224	0.208023	0.583888
						0.5				1.133793	16.590693	124.369802

0.2	0.2	0.2	1	0.1	0.01	0.6	0.1	0.1	3	1.133793	9.244399	93.421411
						0.7				1.133793	-0.008786	7.294585
0.2	0.2	0.1	1	0.01	0.1	0.5	0.5	0.1	3	0.900736	-0.196832	2.784835
							0.7			0.900719	-0.408475	3.676835
							0.9			0.900713	-0.622185	4.581861
0.2	0.2	0.1	1	0.01	0.1	0.3	0.01	0.5	3	0.900707	0.142261	1.559958
								0.7		0.883343	0.075542	1.965902
								0.9		0.881718	-0.013030	2.452366
0.2	0.2	0.1	1	0.01	0.1	0.4	0.01	0.1	3	0.890481	0.295498	0.737873
									6	0.883105	0.297615	1.423358
									9	0.882011	0.297900	1.919994

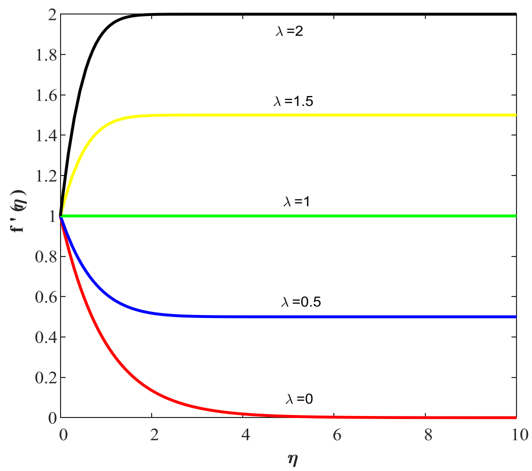

Figure 2 the effect of λ on the velocity profile.

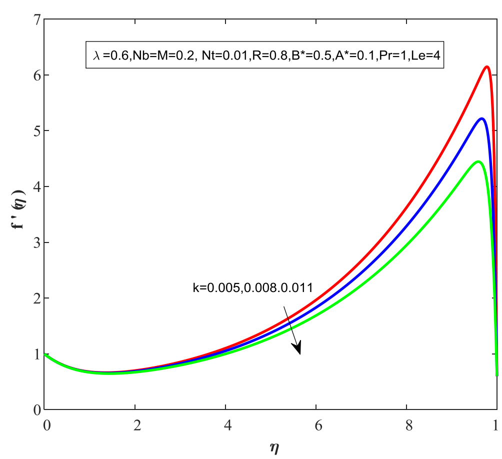

Figure 3a the influence of k on the velocity profile

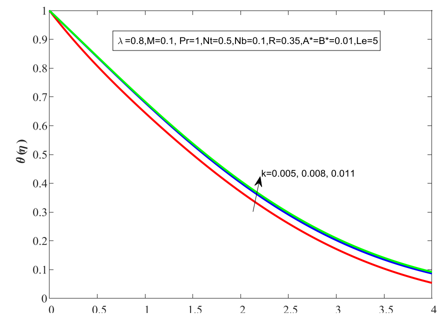

Figure 3b the influence of k on temperature

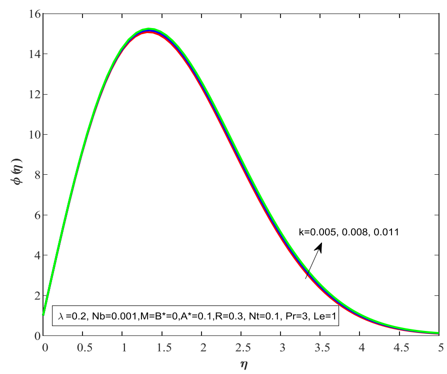

Figure 3c the variation of concentration profiles for different values of k.

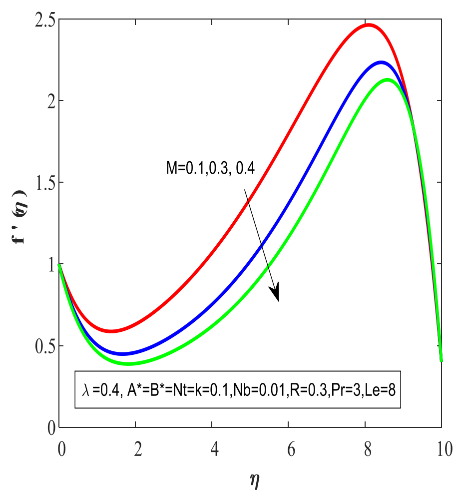

Figure 4a the effect of M on the velocity profile.

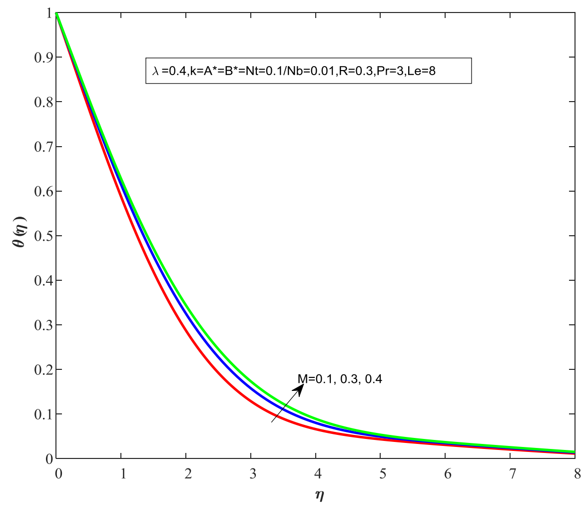

Figure 4b the impact of M on the temperature profile.

For $\lambda = \frac{b}{a} < 1$ i.e. the velocity of the stretching surface is greater than the free stream velocity, the velocity of the fluid and the boundary layer thickness magnify with the upgrade of λ
To the contrary the flow velocity increases and the boundary layer thickness drops with the enlargement of λ when the free stream velocity is larger than the velocity of the stretching surface (i.e. $\lambda = \frac{b}{a} > 1$). In the third case where the two velocities are equal, there is no boundary layer thickness of the nanofluid near the surface as it is revealed in Fig 2.

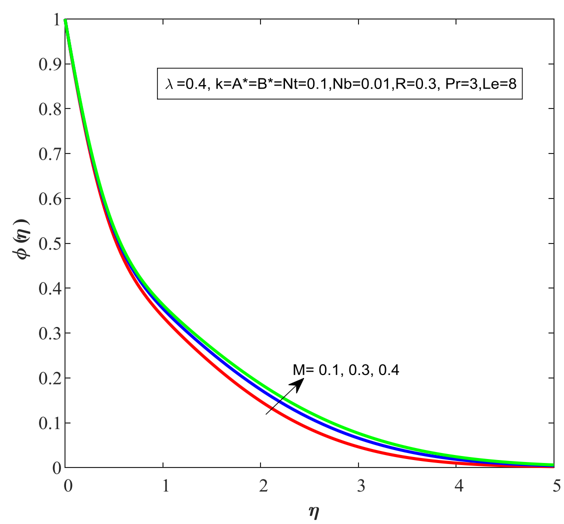

Figure 4c the effect of M on the concentration profile.

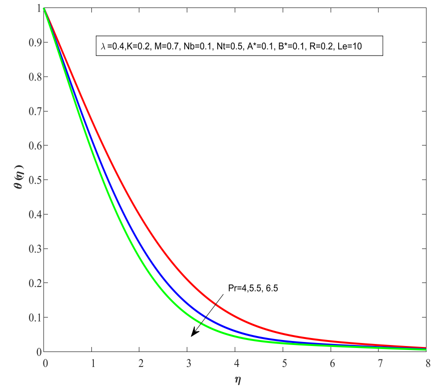

Figure 5 the effect of Pr on the temperature profile.

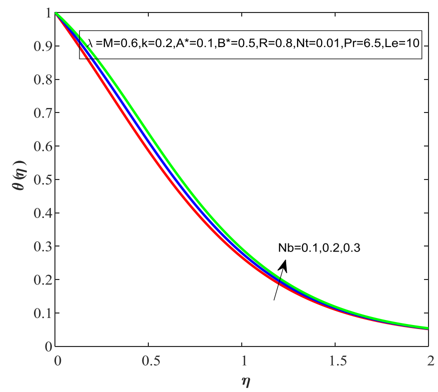

Figure 6 variation of temperature profile for different values of Nb.

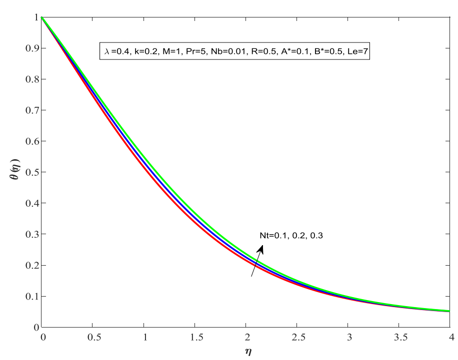

Figure 7 the influence of Nt on the temperature profile.

Increasing the Maxwell parameter k down turn the boundary layer thickness of velocity and upgrade the temperature and the concentration boundary layer thicknesses as it is indicated in Fig 3a, 3b, and 3c respectively. Fig 4a elucidates that the influence of magnetic parameter on velocity. The velocity profile and the boundary layer thickness diminish with the upgrade of M. This is because of the Lorentz force that resists the motion of the fluid whereas the thermal and concentration boundary layers thickness increases with the increase of the magnetic field parameter M as shown in Fig 4b and 4c. The enhancement of the prandtl number reduces the thermal boundary layer thickness. It is due to the smaller the thermal diffusivity the larger the Prandtl number as it is affirmed in Fig 5.

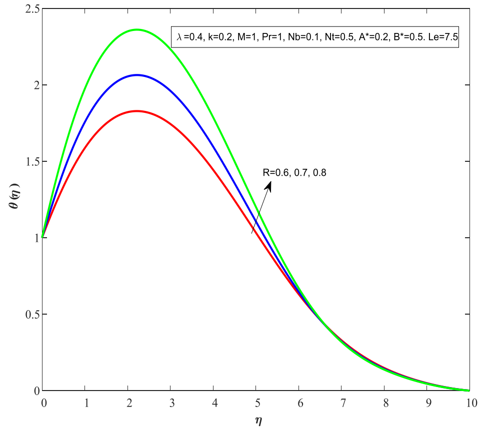

Figure 8 the impact of R on the temperature profile.

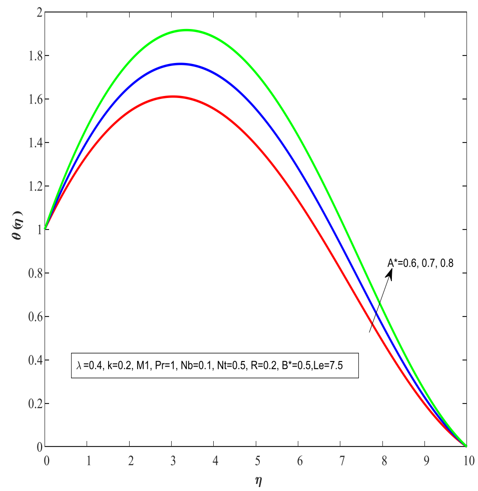

Figure 9 Variation of the temperature profile for different values of A^*.

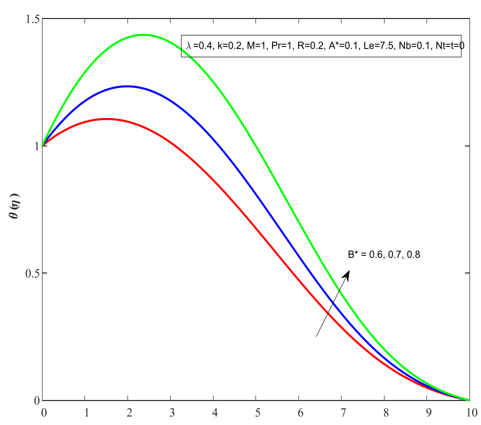

Figure 10 the effect of B^* on the temperature profile.

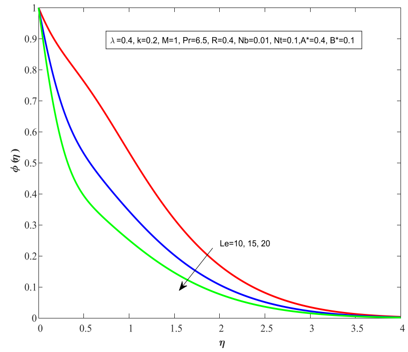

Figure 11 the influence of Le on the concentration profile.

The magnification of the Brownian motion parameter make the thermal boundary layer thicken because the Brownian motion enforce more particles to move from the surface and hence the temperature profile enlarged as it is indicated in Fig 6. Fig7 shows that the increment of the thermophoresis parameter make the thermal boundary layer thickens. Because as Nt increases the thermophoresis diffusion enforce the nanoparticles to move from hot to cold area which enlarges the thermal boundary layer thickness. From Fig 8 it can be seen that increasing the thermal radiation increases the temperature profile and the thermal boundary layer thickens.

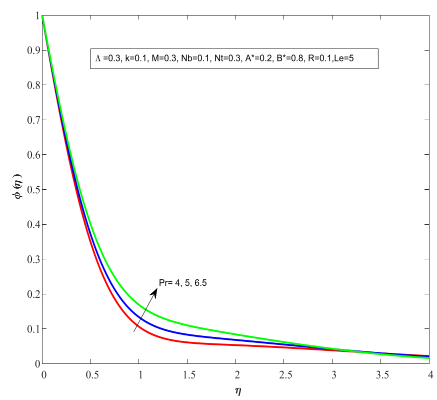

Figure 12 the impact of Pr on the concentration profile.

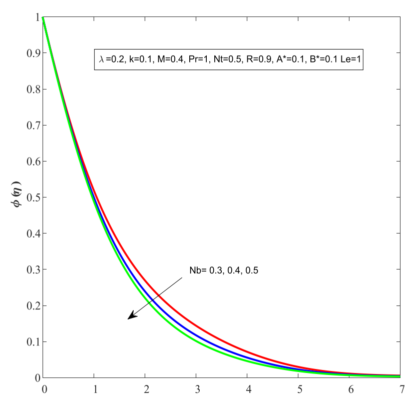

Figure 13 the effect of Nb on the concentration profile.

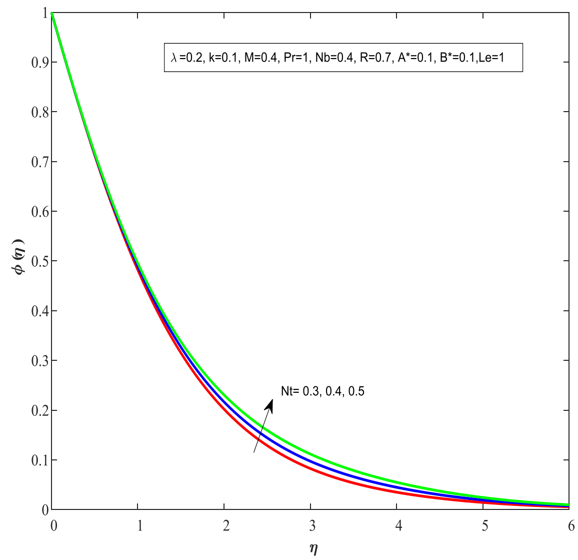

Figure 14 the influence of Nt on the concentration profile.

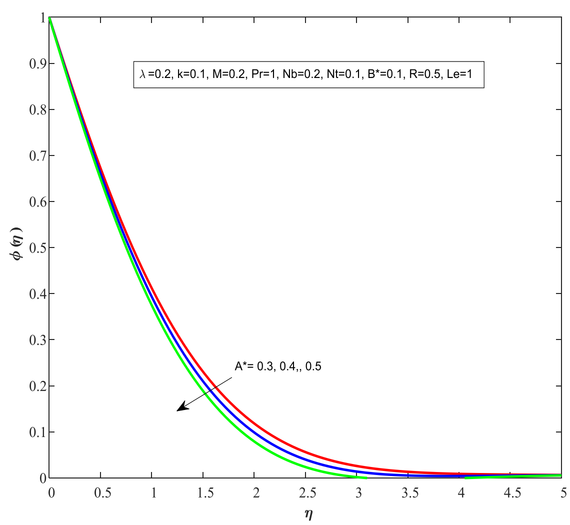

Figure 15 the impact of A^* on the concentration profile.

In Fig 9 and 10, it is revealed that the thermal boundary layer thickness increases with the enlargement of the space and temperature dependent non uniform heat source/sink parameters A^* and B* which corresponds to the internal heat generation that raises the temperature profiles. The molecular diffusivity becomes weaker as the Lewis number increases and the concentration boundary layer becomes thinner as it is illustrated in Fig 11 so that as Le increases the concentration boundary layer decreases. Fig 12 indicates that as Prandtl number increases the boundary layer thickness of the concentration increases.

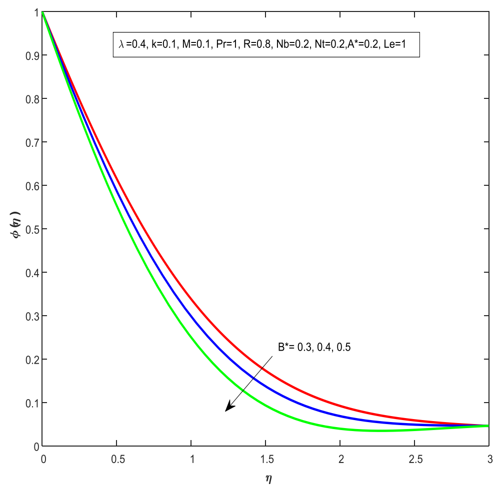

Figure 16 Variation of the concentration profile for different values of B^*.

The concentration boundary layer diminish as the Brownian motion parameter escalated that is revealed in Figure 13, as Nb increases the Brownian motion enforces the nanoparticles transfers the surface heat to the fluid and the nanoparticles gain higher kinetic energy that contributes to the thermal energy of the fluid and cause the movement of the nanoparticles from hot to the cold region. However the concentration boundary layer increases with the increase of Nt as it is shown in Figure 14, increasing the thermophoresis diffusion creates the movement of the nanoparticles from a region of high temperature to a region of low temperature. Figures 15 and 16 reveal that as the space dependent A^* and the temperature dependent B* heat source/sink parameters enhance the concentration boundary layer drops. Because as the nanofluid temperature increase with the increase of A* and B* diffusion of the nanoparticles takes place from high to low temperature regions and hence the concentration boundary layer decrease.

3. Conclusions:

MHD Stagnation point flow of a Maxwell nanofluid over a linear stretching surface with the influence of thermal radiation and non uniform heat source/sink has been studied. Numerical solutions of the governing equations are obtained that permit the computation of the flow, heat and mass transfer behaviors for various values of the velocity ratio λ , the Maxwell parameter k, the magnetic field parameter M, the Prandtl number Pr, the Brownian motion parameter Nb, the thermophoresis parameter Nt, the non uniform heat source/sink space and temperature dependent parameters A^* and B^* as well as the Lewis Number Le. We found the results

1. The velocity boundary layer thickness increases with the increase of the velocity ratio parameter λ but decrease with the magnetic field parameter M and the Maxwell parameter k.
2. Increasing Prandtl number reduces the thermal boundary layer thickness.
3. The thermal boundary layer thickness magnifies with the upgrade of the thermal radiation parameter R, Brownian motion parameter Nb and thermophoresis parameter Nt and similar results have been found for the space dependent and temperature dependent non uniform heat source/sink effects.
4. The concentration boundary thickness enlarges with the increase of the prandtl number Pr and the thermophoresis parameter Nt
5. The escalation of the space dependent parameter (A^*) and the Brownian motion parameter Nb reduces the concentration boundary layer thickness.
6. The concentration Boundary layer thickness diminishes as the Lewis number increases.

References:

[1] Ahmed M. Megahed, Variable fluid properties and variable heat flux effects on the flow and Heat transfer in non Newtonian Maxwell fluid over an unsteady stretching sheet with slip Velocity. Chin.Phy.B. vol.22. N0.9, 2013, (094701-094706).

[2] A.U. Awan, M. Imran, M.Athar and M. Kamran, Exact analytical solution for longitudinal flow of a fractional Maxwell fluid between two coaxial cylinders. Punjab university Journal of mathematics Vol. 45, (2013), Pp9-23.
[3] Dumitru Vieru and Azhar Alizafar. Some coutte flows of Maxwell fluid with wall slip Condition. Appl. Maths. Inf. Sci. 7, No. 1, (2013), 209-219.
[4] Emilia Bozhelkova and Ivan Bazhelkova, Sokes' first problem for viscoelastic fluids with Fractional Maxwell model. Fractal Fract, 2017, 1-12.
[5] G.K. Ramesh, B.J. Gireesha, T. Hayat, A. Alsaedi, Stagnation point flow of Maxwell fluid Towards a permeable surface in the presence of nanoparticles. Alexandria Engineering journal, (2016), 857-865.
[6] G.K. Rammesh, B.J. Gireesha, Influence of heat source/sink on Maxwell fluid over a Stretching surface with convective boundary conditions in the presence of nanoparticles. Ain Shamu Engineering Journal, (2014), 991-998.
[7] Josephe Paullet, Analysis of stagnation point flow of an upper convicted Maxwell fluid. Electronic Journal of differential equations, Vol.2017, No. 302, Pp 1-14(2017).
[8] J.R. Rosenberg and R. Keunings, Further results on the flow of Maxwell fluid through an Abrupt contraction. Journal of non-Newtonian fluid mechanics. Elsvier science publishers, B.V. (1988), Pp, 295-302.
[9] J. Vander Zanden, G.D.C. Kuiken, A. Segal, W. J. Lindhout and M.A. Hussen, Numerical Experiments and theoretical analysis of the flow of an elastic liquid of the upper convicted Maxwell type in the presence of geometrical discontinuities. Applied scientific research, (1985), 303
[10] K.A. Abro, A.A. Shaikh, I.A. Juneio, Analytical solutions under no slip effects for Accelerated flows of Maxwell fluids. Sindh unir.Re Journal (scie. Ser), Vol. 47(3), (2015), 613- 618.
[11] K. Boubaker, An extended Maxwell fluid model interms of dimensionless Relaxation time in polymeric non-Newtonian liquids motion. Frontier in science, 2(3), (2012), 37-40.
[12] Key-Chyang Lee and Bruce A. Finlayson, Stability of the plane poiseuille and couette Flow of Maxwell fluid. Journal of Non-Newtonian fluid mechanics,21,(1986), 65-78.
[13] K. R. Sekhar, G. Viswanatha Reddy C.S.K. Raju. Blasius and Sakiadis flow of MHD Maxwell fluid with exponentially decaying heat source/sink. Iner. Jour. Of research in Science and engineering 2017, Pp, 126-136.
[14] K. Vajravelu, Ronald Li, M. Dewasu rendra,,Joseph Bennaroch, Nicholas Ossi, Ying Zhang, Michael Sammarco, K. V. Parasad. Analysis of MHD boundary layer flow of an upper convicted Maxwell fluid with homogeneous-hetrogeneous chemical reactions. Communication in numerical analysis, No. 2, (2017), 202-216.
[15] Lika Z. Hummady, Ahmed M. Abdulhadi, Peristaltic transport for fractional generalized Maxwell Vscoelastic fluids through a porous medium in an inclined channel with slip effects. Iraq journal of science, Vol. 56, No. 4B, 2015, Pp 3215-3229.
[16] Macha Madhu, Naikoti Kishan, Ali J. Chamkhan, Unsteady flow of Maxwell nano fluid Over a stretching surface in the presence of MHD and thermal radiation effect. Propulsion and power research 6(1), 2017, 31-40.
[17] Meraj Mustefa and Junnoid Ahmmad Khn, Numerical analysis of Sakiadis flow problem Considering Maxwell nanofluid. Journal of thermal science Vol. 21 No. 6B, (2017), Pp, 2747-2756,.
[18] M. Mustefa, Junaid Ahmed Khan, T. Hayat and A.Alsaedi, Sakiadis flow of Maxwell fluid Considering magnetic field and convicted boundary condition. American institute of Physics AIP Advances 5, , (2015), 0271061-9.
[19] M. Qasim and S. Noreen, Falkner-skan flow of a Maxwell fluid with heat transfer and Magnetic field. Inter. Jour. Of engineering mathematics, 2013, 1-7.
[20] Nazila Isahak, Hasmawani Hashim, Muhammad Khairul Anuar Mohammed, Norhafizah M dsarif, Norhayati Rosli, Moha Zukisalleh, Thermal Radiation effects on a stagnation point flow past a stretching/shiriking sheet in a Maxwell fluid with slip condition.IOP conf. Series, Journal of Physics (2017), 1-9.
[21] N. A. Halim, Rizawan UIHug, N.F.M. Noor, Active and passive controls of nanoparticles in Maxwell stagnation point flow over a slipped stretched surface. Meccanica Cross mark (2017), 1527-1539.
[22] N.F.M Noor, Rizwan UI Haq, S. Abbasbandy, I. Hashim, Heat flux performance in porous Medium embedded Maxwell fluid flow over a vertical stretched plated due to heat Absorption. Journal of nonlinear science and applications, (2016), 2986-3001.
[23] Noor Fadiya Mohd Noor, Analysis for MHD flow of Maxwell fluid past a vertical Stretching sheet in the presence of thermophoresis and chemical reaction. Int. Jour. Of Physical and mathematical science Vol. 6, No. 4, 2012, 485-489.
[24] N. Sandeep, C. sulachana, Momentum and heat transfer behavior of Jeffrey, Maxwll and oldroyd B nanofluids past astreching surface with non uniform heat source/sink. Ain Shams Engineering Journal, (2016), 1-8,
[25] Syed Yedulla Qadri,M. Veera Krishna, Run up flow of a Maxwell fluid through a parallel Plate channel. American Journal of computational mathematics 3, 2013,297-303.
[26] Siddique, Exact solution for the longitudinal flow of generalized Maxwell fluid in a circularCylinder. Arch.Mech. 62, 4, warszzawa,(2010), Pp305-317.
[27] Sin Wei Wong, M.A.Omer Awang and Anuar Ishak, Stagnation point flow toward a vertical Non-linear stretching sheet with the prescribed surface heat flux. Journal of applied Mathematics, 2013,1-6.
[28] Sreekala, M Veerakrishna and Kesava Reddy, Unsteady MHD three dimensional flow of Maxwell fluid through porous medium in a parallel plate channel under the influence of Inclined magnetic field. International Journal of Advances in Engineering and Technology, vol. 7, issue 3, 2014, Pp. 1027-1037.
[29] Swati Mukhopadhyay, Upper convicted Maxwell fluid flow over an unsteady stretching Surface embedded in porous medium subjected to suction/blowing. Z. Natureforsch 67a, (2012),641-646.
.[30] Swati Mukhopadhyay, Heat transfer analysis of the unsteady flow of a Maxwell fluid over a stretching surface in the presence of heat source/sink. Chin. Phys. Lette. Vol. 29 No.
5, (2012), 054703-1-054703-4.
[31] T. Hayat, Z. Abbas and M.sajid, MHD stagnation point flow of upper convicted Maxwell f luid over astretching surface. Chaos, solutions and Fractals, , (2009), 840-848.
[32] T. Hayat , S.A. Shehzad and A.Alsaedi, study on three dimensional flow of Maxwell fluid over a stretching surface with convicted boundary conditions. Inter. Jour. Of physics science vol. 7(5), 2012, Pp. 761-768.
[33] Vijendra Singh and Shweta Agarwal, MHD flow and heat transfer for Maxwell fluid over an exponentially stretching sheet with variable thermal conductivity in porous medium.Thermal science vol.18, supple.2, (2014), Pp S599-S615.
[34] Z. Abbas, Y.wang, T.hayat, M.Oberlack, Mixed convection in stagnation point flow of Maxwell fluid towards a vertical stretching surface. Non linear analysis: Real world applications.11, (2010), 3218-3228.